A techno-economic analysis of thermochemical pathways for corncob-to-energy: fast pyrolysis to bio-oil, gasification to methanol and combustion to electricity

George Victor Brigagão[1], Ofélia de Queiroz Fernandes Araújo[1], José Luiz de Medeiros[1], Hrvoje Mikulcic*[2], Neven Duic[2]

[1] Escola de Química, Federal University of Rio de Janeiro, CT, E, Ilha do Fundão, Rio de Janeiro, RJ, 21941-909, Brazil

[2] Department of Energy, Power Engineering and Environment, Faculty of Mechanical Engineering and Naval Architecture, University of Zagreb, Luciceva 5, HR-10000 Zagreb

*Corresponding Author, hrvoje.mikulcic@fsb.hr

Other e-mails: george.victor@poli.ufrj.br (G.V. Brigagão), jlm@eq.ufrj.br (J.L. de Medeiros), ofelia@eq.ufrj.br (O.Q.F. Araújo), neven.duic@fsb.hr (N. Duic)

Abstract

Global warming concerns have driven developments in carbon neutral energy, pulling initiatives on biofuels production. However, the low bulk density and low specific energy of biomass refrain its widespread use due to logistic costs comprising harvesting and collection, storage, pretreatments and transportation. This work approaches increasing land energy productivity by thermochemical conversion of residual biomass to energy products, identifying the best options in terms of energy efficiency and economic indicators. Techno-economic performance of three corncob-to-energy pathways are investigated: gasification to methanol, fast pyrolysis to bio-oil and combustion to electricity. Fast pyrolysis allows higher energy recovery in its products (79%) than biomass gasification to methanol (53%), with biomass densification (volume reduction) of 72.7% and 86.2%, respectively. The combustion route presents net efficiency of 30.2% of biomass low heating value (LHV). All alternatives are economically feasible provided biomass cost is lower than US$75.5/t. The minimum allowable product prices for economic attractiveness of gasification, combustion and

pyrolysis routes are US$305/t methanol, US$80.1/MWh electricity and US$1.47/gasoline-gallon-equivalent bio-oil. Despite its vulnerability to price volatility, gasification presents the highest net present value, seconded by the combustion route, which has lower medium-term payback and investment than gasification due to its process simplicity.

Keywords: corncob; thermochemical conversion; biomass pyrolysis; biomass gasification; methanol synthesis; cogeneration.

1. Introduction

Expansion of the world energy demand and global warming concerns have driven developments of carbon neutral energy sources, pushing production of transportation fuels from biomass [1]. Carbon neutrality of biofuels has been challenged, as carbon stock decreases with land use changes. Thus, harvesting for biofuels demands energy conversion efficiency and increased productivity [2].

A promising alternative for increasing energy productivity is the use of agricultural waste to produce electricity, as occur in the sugarcane-based bioethanol industry, where heat and electricity are co-generated from bagasse [3], with significant improvements in energy efficiency [4]. The same applies to corn-ethanol industry, where co-generation has been also suggested to improve its competitiveness over Brazilian sugarcane-ethanol [5]. Among the corn residues (cobs, husks, leaves and stalks), cobs stand out with reduced mineral [6] and nitrogen contents [7], favoring its utilization for combustion applications [6] and biofuels production. Although corncobs are mostly left to decay in the fields after grain harvests [7], energy products from corn residues have received increasing attention, e.g. electricity and products from thermochemical pathways, e.g. pyrolysis to biochar [8] and gasification to dimethyl ether [9] and methanol [10].

Comprising harvesting and collection, storage, pretreatments and transportation, biomass logistics costs refrain its widespread use in electricity and biofuels production [11]. Gallagher et al. [5], for the case of corn-processing regions, considered geographical location as critical for investing in biofuels, not only for the distance but also for the absence of trade barriers. Additional drawbacks in biomass utilization are its variability (chemical composition and physicochemical properties) and low bulk density, which is overcome by biomass densification [12], allowing higher energy density (i.e. increased volumetric calorific value), thus reducing logistics costs.

Pelleting and briquetting are common densification alternatives being an important issue the ability of the densified biomass to remain intact when handled during storage and transportation. Preheating or steam conditioning of the raw biomass increases durability (i.e. physical strength and mechanical resistance) and can have a significant effect on the calorific value of the pellet and briquet [13]. Briquetting or pelleting corncobs can increase its bulk density to ≈550 kg/m³ [6], which means halving the grinded corncob volume. Torrefaction, or mild pyrolysis (at 200-300°C), enhances biomass properties (e.g., lower water content and increased heating value), producing a dry carbonaceous solid, where 70% of initial weight and 80-90% of original energy are obtained, reducing logistics costs and can be a pretreatment process prior to pelleting [13].

The recovery of energy from biomass is moving from pelleting and briquetting towards biochemical and thermochemical processes. Besides yielding a wide range of products, replacing their original fossil source, thermochemical processes are flexible with respect to the variety of biomass feedstock [14]. Among thermochemical routes, pyrolysis has higher flexibility as process conditions (temperature, heating rate and residence time) can be optimized to maximize the production of targeted products [15]. It is a promising thermochemical conversion, which decomposes biomass into solid biochar, liquid bio-oil,

and combustible gas to meet different process goals [16]. Fast pyrolysis is employed to maximize bio-oil production and occurs at very high heating rates, temperature of ≈500°C, short vapor and char residence times and rapid cooling of pyrolysis vapor [17], while slow pyrolysis applies low heating rate, moderate temperature (≈400°C) and high residence time to favor bio-char production [15]. Fast pyrolysis bio-oil has increased energy density, ≈6.5 fold increase over raw biomass, halving land area requirements for fuel storage and handling, compared to solid fuel handling systems [18].

Bio-oil direct use as fuel presents difficulties due to its high viscosity, poor heating value, corrosiveness, and instability [19]. Hence, bio-oil requires upgrading into naphtha-range transport fuels, which is obtained via two major conventional refinery operations – hydroprocessing and catalytic cracking processes [20], with hydrotreatment under mild conditions (150–450 °C, 50 bar) being one of the main routes [21]. The key to bio-oil upgrading is to remove oxygen with minimal hydrogen consumption, while retaining its carbon content [22]. A comprehensive review concerning the challenges of bio-oil production and upgrading is provided by Sharifzadeh et al. [23]. A review on the methods used for detailed simulation of fast pyrolysis reactors via computational fluid dynamics is addressed by Xiong et al. [24], which discussed in a later work [25] the trends and major barriers for accurate reactor-scale predictions.

Trippe et al. [26] approached fast pyrolysis for a decentralized fuel production chain, saving in transportation costs due to increased energy density of crude bio-oil mixed with pulverized bio-char (biosyncrude). In fact, the low energy density of raw biomass constrains its transportation to short distances, contrasting with biomass-to-liquids (BTL), which is suitable for large scale facilities. In the business model of Trippe et al. [26], multiple decentralized pyrolysis plants are built to obtain biosyncrude that can be economically transported over

long distances to a centralized large scale processing unit [26]. Alternatively, modular and transportable bio-oil plants can be built close to the biomass sources [18].

Experimental work on corncob fast pyrolysis by Zhang et al. [27] employed a bubbling fluidized bed reactor fed with pure nitrogen to investigate performance sensitivity to experimental factors, among which the reaction temperature and particle size. In later work [28], catalytic fast pyrolysis was approached unveiling the existence of a trade-off between bio-oil quantity (yield) and quality (composition or heating value). Zhang et al [29] presented the effects of using different carrier gases on product gas of corncob fast pyrolysis.

Competing with fast pyrolysis, biomass gasification occurs at higher temperatures (700-1000°C) and necessarily with addition of a gasifying agent [30] – generally steam, air or oxygen (O_2) – yielding product gas containing carbon monoxide (CO_2), carbon dioxide (CO), hydrogen (H_2), methane (CH_4), aliphatic and aromatic light hydrocarbons, tar and water. [31]. Product gas has use in co-generation, thermal cracking or catalytic reforming to yield syngas with reduced hydrocarbon content [32].

Syngas is a versatile building block in the chemical industry, with main use in the synthesis of ammonia ($\approx$55%), H_2 supply to oil refining processes ($\approx$24%), and, to a smaller extent, for methanol production (12%) [32]. Other products derived from syngas are Fischer–Tropsch (FT) fuels, ethanol and synthetic natural gas [1]. FT reaction produces a variety of linear and branched-chain synthetic hydrocarbons [33] while methanol, besides having use as fuel, is a major energy carrier and an important chemical commodity [34].

Anex et al. [35] performed a techno-economic comparison of alternatives for corn stover processing including gasification to FT liquids, fast pyrolysis to bio-oil and biochemical conversion to ethanol (second generation). The authors evaluated the product values for project attractiveness, concluding that pyrolysis has the best economic performance and

biochemical conversion the worst. Zhao et al. [36] employed Monte Carlo simulation to compare on economic grounds pathways to produce ethanol and synthetic hydrocarbons, showing that fast pyrolysis of corn stover would be preferred by risk-averse investors.

Regarding the use of corncobs, a literature gap exists in-techno-economic comparisons of production routes to bio-oil, methanol and electricity. A review by Brown et al. [37] covering the economic performance of thermochemical pathways to biofuels production included a critical discussion of the major assumptions adopted in the literature. The authors emphasize fixed capital investments and minimum allowable product prices for economic attractiveness.

In this work, gasification of biomass to syngas and its final destination to methanol is compared to fast pyrolysis as biomass energy densification route producing bio-oil. Both alternatives have as competitor the direct combustion of biomass in power plants. The original contribution is to fulfill the identified literature gap on comparative techno-economic analyses of these thermochemical alternatives for conversion of corncob, an agricultural waste abundantly available in the USA. The relevance of the contribution is the context of energy densification of waste biomass for its efficient use and transportation as energy feedstock. Combustion is taken as a reference project, due to its widespread use in biomass-fired steam power plants, and for being supplier of electricity and heat in fast pyrolysis and gasification alternatives. The analysis methods involve process simulation in Aspen HYSYS allowing rigorous thermodynamic models and equipment representation to calculate energy and mass balances for the three processes: fast pyrolysis to bio-oil (PYROL), gasification to methanol (GASIF) and combustion to electricity (COMB). Composition characterization of corncob biomass is presented, with description based on model molecules from experimental results reported in the literature [29]. Simulation results support calculation of energy efficiency, equipment sizing and economic analysis. Sensitivity analysis of economic performance to prices of corncob feedstock and products is presented.

2. Methods

Techno-economic evaluation of the three investigated process alternatives (GASIF, PYROL and COMB) is performed based on the block diagrams depicted in Fig. 1.
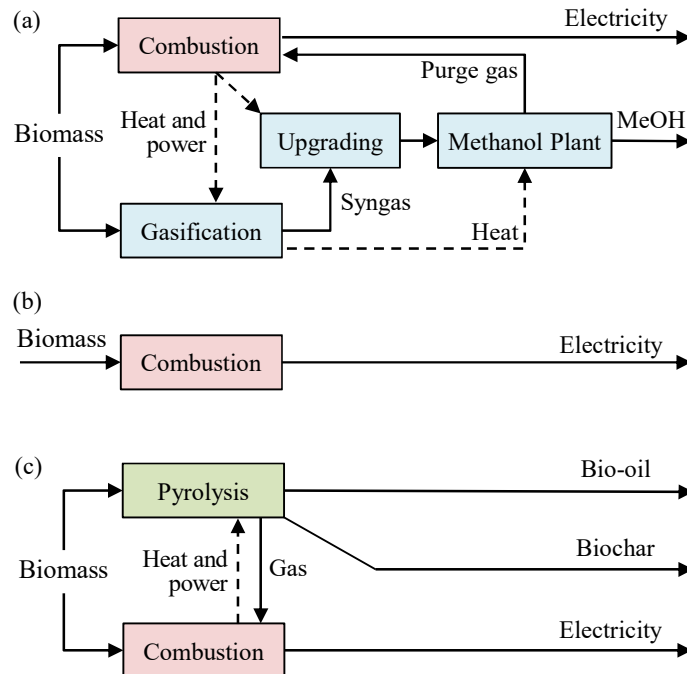

Fig. 1. Alternatives for energy densification of corncob biomass through thermochemical processes: (a) methanol production through gasification; (b) combustion for power generation (COMB); and (c) pyrolysis for bio-oil. Gasification and pyrolysis employ partial use of biomass in auxiliary combustion process to supply process electricity and heating demands, exporting surplus electricity.

2.1. Processes Description

The operational conditions and the main aspects of the three thermochemical routes – GASIF (Fig. 1a), COMB (Fig. 1b) and PYROL (Fig. 1c) – are addressed. The process alternatives are equally fed with 96.81 t/h (94.48 t/h on ash-free basis) of corncob biomass grinded with particle size from 1 to 2 mm [27, 29].

2.1.1. Biomass Gasification

GASIF process flowsheet (Fig. 2) uses syngas to produce methanol, with surplus gas used with biomass co-firing for combined heat and power generation. Table 1 summarizes process conditions and assumptions for biomass gasification and raw syngas cooling.
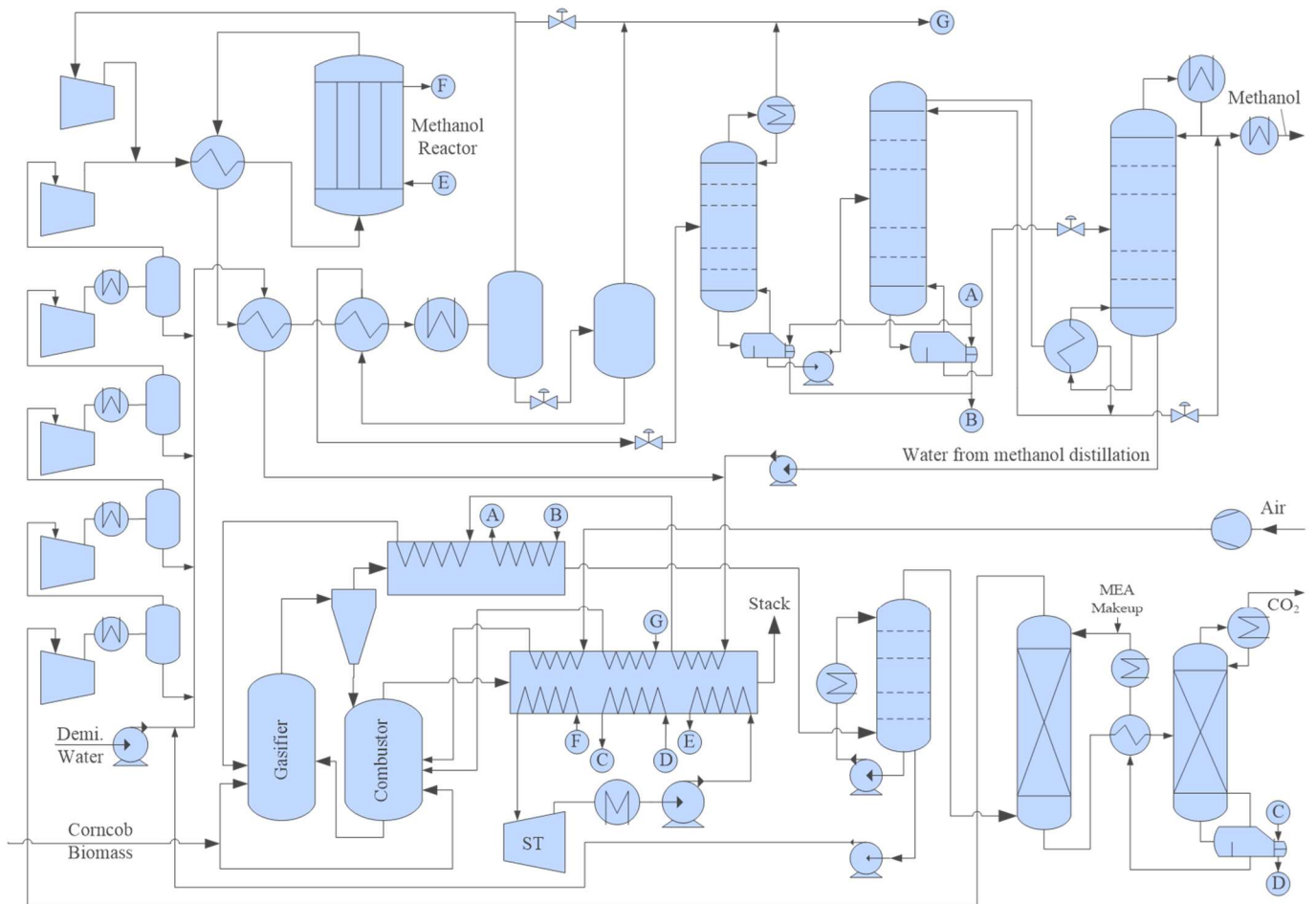
Fig. 2. Process flowsheet of biomass gasification to produce methanol (GASIF).

Table 1. Premises and conditions for biomass gasification and raw syngas cooling.

Item	Value	Unit
Biomass feed (ash-free basis)	58.61	t/h
Steam feed rate	58.56	t/h
Steam temperature	250	°C
Syngas temperature	900	°C
Syngas pressure	3.00	bar
HRSG (heat recovery steam generation) boiler pressure	3.25	bar
HRSG gas pressure drop	5.0	kPa
HRSG gas outlet temperature	180	°C
DCC (direct contact column) gas outlet temperature	35.4	°C
DCC pressure drop	10	kPa
DCC theoretical stages	04	-

A circulating fluidized bed gasifier is employed, with the reaction heat supplied by hot sand

provided by biomass combustion. Corncob particles are conveyed to the gasifier with

superheated steam at 3 bar and 250°C (1:1 mass ratio) and feed of 58.61 t/h (ash-free basis);

the remaining 35.87 t/h is used for combustion to supply internal heat demand. Raw syngas (mainly H_2, CO and CO_2) leaves the gasifier at 900°C and goes to a heat recovery steam generator (HRSG), where superheated steam utilized in gasification is produced and saturated water at 3.25 bar is boiled to supply heat demand of the methanol purification section (distillation column reboilers). To minimize condensation of tar compounds in HRSG and associated issues such as corrosion and fouling [38], hot syngas exits HRSG at 180°C, with the finishing cooling being performed in a plate direct contact column (DCC) cladded with stainless steel, fed with cold condensate recycled from column bottom. The condensate purge is used to minimize demineralized water consumption, being mixed with other residual aqueous streams in the plant, obtained from condensate drums of the syngas compressor. The condensate mixture is reheated to generate superheated steam to the gasifier.

The cooled raw syngas leaves the DCC at 35.4°C requiring adjustment of the proportion of components H_2, CO and CO_2 to ideal stoichiometric conditions for methanol synthesis, expressed by S coefficient close to 2.0, as defined by Eq. (1), where the brackets express the molar contents.

$$S = \frac{[H_2] - [CO_2]}{[CO] + [CO_2]}$$

(1)

The targeted S value is reached via CO_2 removal by chemical absorption with aqueous monoethanolamine (MEA) at 20%w/w. Syngas at 2.5 bar leaves at the top of the absorber with 2.53%mol CO_2 (wet basis). Table 2 provides process conditions and premises for simulation of syngas upgrading.

Absorber bottoms (CO_2-rich MEA) flows to the regeneration column, where CO_2-rich gas at 1.8 bar (4.17%mol H_2O) leaves at the top with 99.89%mol CO_2 dry-basis purity. Heat integration of lean and rich solvent streams minimizes heat load to the column´s reboiler. It is worth noting that 39.78% of corncob mass flow is carbon and 22% of this amount leaves

9

the MEA regeneration column as practically pure CO_2 (CO_2-rich gas). It could be monetized

after intercooled compression stages, through pipeline dispatch, as a high-pressure liquid or,

by truck, as cryogenic liquid (or even as dry-ice). Besides contributing to process revenues

from its commercialization, this CO_2-rich gas could be used as enhanced oil recovery agent.

This would characterize the entire process as a negative CO_2 emitter, i.e. a bio-energy with

carbon capture and storage (BECCS) technology. With BECCS, CO_2 storage could contribute

to process profitability by considering a cap-and-trade scenario. For the sake of simplicity,

destination of this CO_2-rich gas is not considered in this work.

Table 2. Premises and conditions for CO_2 removal in syngas upgrading.

Item	Value	Unit
Solvent	20	%w/w aq. MEA
Lean MEA	1.25	%mol CO_2
Capture-Ratio	17	kg solvent/ kg CO_2
Absorption stages	15	-
Absorption pressure drop	35	kPa
Absorption top pressure	2.50	bar
CO_2 in lean gas	2.53	%mol CO_2
Regeneration stages	10	-
Regeneration pressure drop	10	kPa
Regeneration top pressure	1.80	bar

Table 3 summarizes the main premises and conditions related with methanol production.

Table 3. Premises and conditions for methanol production.

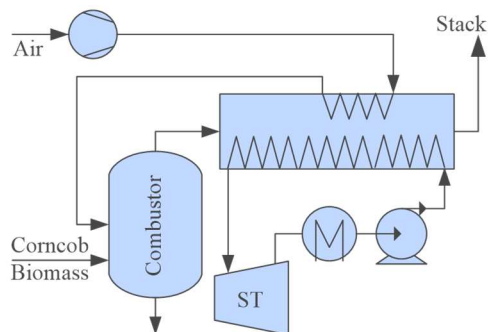| Item	Value	Unit
Methanol synthesis (reactor)		
Inlet pressure	60	bar
Inlet temeprature	240	°C
Outlet temeprature	260	°C
Purification (distillation columns)		
Column#1 condenser temperature	40	°C
Column#2 condenser temperature	119.5	°C
Column#3 reboiler temperature	109.9	°C
Methanol purity	99.85	%w/w

Syngas from MEA absorption presenting *S=2.018* is sent to five-stage compression before entering the methanol synthesis loop at ≈60 bar. The methanol reactor has a steam raising design, configuring a shell and tube heat exchanger, and tubes packed with catalyst (methanol synthesis). It is simulated as an equilibrium reactor, fed with a mixture of fresh syngas and recycled unreacted gas at 240°C. The reaction heat is recovered through steam generation in the shell side at 230°C (≈28 bar). The amount of catalyst required is calculated accordingly to typical weight-hourly-space-velocity of 3 h^{-1}. The product outlet at 260°C is firstly cooled down to 107°C in a battery of exchangers to: (i) heat the reactor feed gas; (ii) preheat the water stream for gasifier feed; and (iii) reheat the low-pressure raw methanol sent to purification. Then it is finally cooled down to 40°C for condensation of raw methanol, leaving substantial amount of tail gas, from which 10% is withdrawn as purge gas, with the other 90% being recycled to reactor feed. Raw methanol is expanded to ≈4 bar producing a small fraction of gas that is mixed to the purge gas from the synthesis loop. The liquid is then reheated (cooling reactor product) prior to entering the first distillation column to minimize reboiler duty, whereas the purpose of the first distillation column is the removal of light compounds (e.g. dissolved gases). The overhead vapor is mixed to the purge gas and sent to the combustion furnace for co-firing with corncob biomass, supplying 20% of its energy demand. The bottom methanol-water mixture is pumped to the next distillation column at ≈6.5 bar, where ≈45% of methanol is recovered at the top as commercial grade product (99.85%w/w). The third column finishes the methanol-water fractionation, operating at nearly atmospheric pressure, with the reboiler duty supplied by heat integration with condensation of pressurized methanol vapor from the top of the second column.

Corncob co-firing (35.87 t/h) with purge gas (6.56 t/h) is performed with 10% excess air producing hot sand for gasification and hot gas at 1050°C for another HRSG section, where exhaust gas heat is recovered by several process streams and cooled to 95°C: (i) air feed; (ii)

purge gas feed; (iii) non-saturated water that is subsequently heated in other HRSG to produce superheated steam to gasification; (iv) low-pressure saturated water to supply MEA reboiler with steam; (v) water and saturated steam at ≈28 bar for power generation, with latent heat being supplied by methanol synthesis reaction heat. After pressurized to 28.2 bar, water of Rankine cycle is pre-heated to saturation in exhaust gas HRSG and then sent to boil up in the methanol reactor; produced saturated steam returns for superheating. The steam turbine (ST) is fed with superheated steam at 560°C and 27.7 bar generating electricity for the plant, mostly to drive the syngas compressor, with the exceeding power (3.7 MW) being exported. The Rankine vacuum condenser operates at 0.096 bar and 45°C.

2.1.2. Biomass Combustion

Fig. 3 shows the process flowsheet of the biomass combustion route, which is totally based in electricity generation in a corncob-fired Rankine cycle. Despite not indicated in Fig. 3, heat recovery also occurs in the furnace radiation zone to generate superheated steam for the turbine. Able to export 114.10 MW of electricity, the estimated power plant net efficiency is 30.2%LHV. Major assumptions and process conditions are shown in Table 4. Contrarily to the biomass gasification route, implementation of BECCS in this case would require CO_2 removal from diluted (N_2-rich) flue gas, a rather expensive operation.

Fig. 3. Process flowsheet of biomass combustion to produce electricity (COMB).

Table 4. Operating conditions of the power generation process.

Item	Value	Unit
Biomass feed rate	96.81	t/h
Excess air for combustion	10.0	%
ST adiabatic efficiency	90.0	%
ST inlet temperature	560	°C
ST inlet pressure	27.70	bar
ST outlet pressure	0.096	bar
Condenser outlet temperature	45.0	°C

The ST is fed with superheated steam at 560°C and 27.7 bar. The Rankine vacuum condenser also operates at 0.096 bar and 45°C. After being pumped to 28.2 bar, a fraction of pressurized water is sent to the furnace (not shown) and another fraction is sent to exhaust gas HRSG. The exhaust gas is assumed to enter the HRSG at 1050°C, and then released to the atmosphere at 100°C through the stack.

2.1.3. Biomass Fast Pyrolysis

Biomass fast pyrolysis route considers exportation of raw bio-oil (i.e., without further treatment or upgrading), with exceeding non-condensable gas availed for combined heat and power generation with biomass co-firing. Bio-oil upgrading, stabilization or fractionation for recovery of valuable chemicals is assumed to be performed in a centralized (high capacity) chemical plant or oil refinery, where H_2 is readily available to be utilized for bio-oil hydrotreating. Consequently, the capital investment is drastically minimized. It is worth noting that this alternative involves the lowest capacity machines (turbines, compressors and pumps) in comparison with the other evaluated routes.

The process flowsheet of the biomass pyrolysis route is presented in Fig. 4, while process conditions and premises are shown in Table 5.

Fast pyrolysis yields and bio-oil composition are based on experimental results of Zhang et al. [29]. Corncob particles are conveyed to the pyrolysis reactor where they are fluidized with

recycled non-condensable gas. The biomass feed rate is 82.88 t/h, while the remaining 11.60

t/h is burnt for supplying the pyrolysis heat demand.

Hot vapor at 550°C and 1.46 bar goes from the fast pyrolysis reactor to solids collection (with

assumed 100% efficiency). It is then cooled in a battery of three plate-based DCCs (04

theoretical stages each) quenched with the recycle of cooled bio-oil condensate. Quick

cooling after dust removal aims to rapidly cease chemical reactions, besides minimizing

fouling and facilitating cleaning [17].
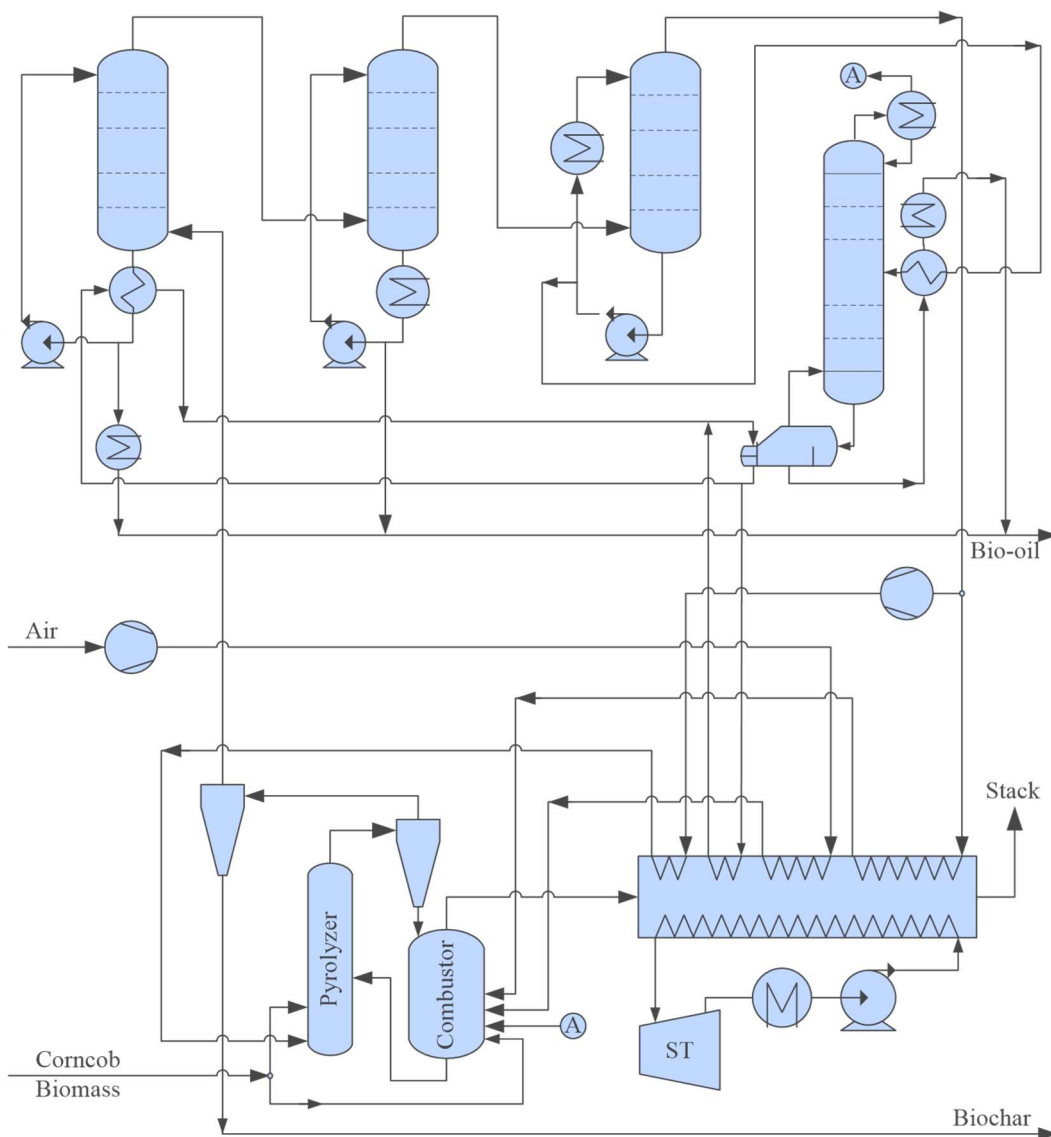
Fig. 4. Process flowsheet of biomass pyrolysis for bio-oil production (PYROL).

In the first DCC, hot vapor at 550°C is cooled to 198°C by heavy bio-oil at 185°C recycled from column bottoms. This overhead vapor is connected to the bottom of the following DCC, which is fed by the top with a lighter fraction of bio-oil at 40°C, also recycled from column bottoms, that cools the vapor feed down to 103°C. Finally, this vapor enters the third DCC to be cooled down to 42°C. About 57% of the gas leaving the top of DCC#3, consisting mainly of CO_2, CO, H_2 and CH_4, is directed to combustion, with the remaining part being recycled to the pyrolysis reactor.

Table 5. Biomass fast pyrolysis conditions and premises.

Item	Value	Unit
Biomass pyrolysis		
Corncob feed rate (ash-free basis)	82.88	t/h
Operating temperature	550	°C
Outlet pressure	1.46	bar
Pressure drop	20	kPa
Product cooling		
DCC#1 liquid inlet temperature	185	°C
DCC#1 gas outlet temperature	198	°C
DCC#1 pressure drop	10	kPa
DCC#2 liquid inlet temperature	40	°C
DCC#2 gas outlet temperature	103	°C
DCC#2 pressure drop	10	kPa
DCC#3 liquid inlet temperature	40	°C
DCC#3 gas outlet temperature	42	°C
DCC#3 pressure drop	10	kPa
Distillation		
Water content at bottom product	9.62	%w
Water content at top waste vapor	99.3	%w

As bio-oil is expected to be highly acidic and corrosive (pH≈3), the DCC columns are cladded with stainless steel. Hot heavy bio-oil leaves the bottom of DCC#1 at 237°C and is cooled to 185°C recovering heat to generate saturated steam, to partially supply a distillation reboiler. In the case of DCC#2, bottom liquid at 116°C is cooled to 40°C. Both in DCC#1 and DCC#2, the fraction of bottom liquid that is not recycled is sent to a product header. DCC#3 operates below 100°C producing condensate at 82°C with very high water content

(71.3%w), which is sent to distillation for recovery of organic compounds. A bio-oil header receives the different fractions produced in DCC#1 and DCC#2, in addition to the light compounds recovered via distillation. The reboiler heat duty is mostly supplied with steam generated from heavy bio-oil cooling at the bottom of DCC#1, which is complemented by saturated steam generated through exhaust gas heat recovery.

Corncob co-firing (11.60 t/h) with pyrolysis gas (16.42 t/h) employs 10% excess air, producing hot sand for pyrolysis and hot gas at 1020°C for a HRSG section, where several process streams are heated while the flue-gas cools down to 100°C: (i) air feed; (ii) pyrolysis gas for combustion; (iii) pyrolysis gas for recycle; (iv) low-pressure saturated water (to supply steam to the distillation reboiler); and (v) Rankine cycle streams. Biomass, air, pyrolysis gas and 15.37 t/h of water vapor (99.3%w/w) from distillation column (avoiding the need of residual water treatment) is sent to the combustor to convert organic compounds. As the pyrolysis plant has low electricity consumption, the ST power is mostly exported (7.85 MW). The ST is also fed with superheated steam at 560°C and 27.7 bar.

2.2. Simulation of Process Alternatives

Process alternatives are simulated in Aspen HYSYS 8.8 using Peng-Robinson Equation-of-State (PR-EOS) with exception of free-water/steam systems that use NBS Steam. For liquid phase containing organic compounds, other thermodynamic models are applied: Cubic Plus Association EOS for high-pressure applications (methanol synthesis loop); UNIQUAC liquid-phase activity coefficient model coupled to PR-EOS vapor-phase for low-pressure systems (biomass pyrolysis and methanol purification), with UNIFAC group contribution method employed to estimate missing binary interaction parameters; and Acid-Gas Package for CO_2 chemical absorption plant.

Biomass is represented by a mix of model substances to reproduce the empirical elemental composition given by Zhang et al. [29], expressed as reduced chemical formula to $CH_{1.554}N_{0.006}O_{0.824}$ (excluding H_2O), with given 8.64%w/w humidity and 2.41%w/w ash (LHV=16.19 MJ/kg, dry ash-free basis). Several substances available in HYSYS component database were tested for this purpose. The candidate molecules were selected considering their LHV value, allowing representation of biomass, lignite and coal.

The mix is represented by a minimum number of components that satisfies the given reduced chemical formula and meets the following original set of heuristics: (H1) a sugar compound should be the base component, as it presents the closest proportions of chemical elements; (H2) a hydrocarbon of conjugated aromatic rings may be included to increase the element ratios C/H and C/O; (H3) an oxygenated compound of low hydrogen content should be included to balance C/H and C/O ratios; (H4) a nitrogen-containing cyclic molecule should be included and cyclic molecules are desirable to increase the calorific value of the mixture; (H5) molecular weights should be as high as possible to mimic a biomolecule.

For each trial combination of selected model compounds, a set of linear equations were algebraically solved to determine the composition that matches the biomass overall reduced formula. Then, the compositional model of the biomass is validated against the obtained LHV [29]. Following the given guidelines, 20 combinations were tested. Only the mixture showing the best LHV agreement is reported.

Milling power requirement of corncob gridding to produce small particles is not included in the analysis, as it is supposed to be performed by biomass suppliers to improve storage and transportation efficiencies. Additionally, since the three evaluated processes require small sized particles, the gridding operation does not discriminate the alternatives, being excluded from the analysis.

Gasification is simulated with HYSYS Gibbs reactor model, neglecting generation of tar

compounds [39], so that syngas production is estimated at its thermodynamic limit.

Conversely, since fast pyrolysis products are essentially dependent on kinetic control of

chemical reactions, the yields are guided by the experimental results of Zhang et al. [29],

which reported different bio-oil compositions for various fluidizing gases, with the assumed

product yields presented in Table 6. The bio-oil fraction is modelled with composition shown

in Table 7 using model components for representing each group of substances in accordance

with the main compounds obtained by Zhang et al. [29].

Table 6. Biomass pyrolysis yields (ash-free).

Item	Yield (%), mass-basis
Gas	19.00
H_2	0.112
CO	6.290
CO_2	11.834
CH_4	0.763
Biochar	26.90
Bio-oil	31.60
Water	22.50

Table 7. Assumed organic composition representative of bio-oil produced by fast pyrolysis.

Chemical Group	Model Component	Chemical Formula	Mass Fraction
Acids	Acetic acid	$C_2H_4O_2$	0.152
Alcohols	2-Furanmethanol	$C_5H_6O_2$	0.034
Aldehydes	Furfural	$C_5H_4O_2$	0.079
Esters	1,2-Ethanediol diacetate	$C_6H_{10}O_4$	0.041
Ethers	Methyl-phenyl ether	C_7H_8O	0.025
Ketones	Hydroxyacetone	$C_3H_6O_2$	0.172
N-containing	2-Pyrrolidone	C_4H_7NO	0.033
Phenols	1,2-Benzenediol	$C_6H_6O_2$	0.285
Sugars	Levoglucosan [a]	$C_6H_{10}O_5$	0.089
Others	2,3-Dihydro-benzofuran [b]	C_8H_8O	0.040
	Water	H_2O	0.050

[a] Levoglucosan ($C_6H_{10}O_5$) is simulated cloning glucose properties
[b] 2,3-Dihydro-benzofuran (C_8H_8O) is simulated cloning acetophenone properties

2.3. Economic Assumptions

The construction site is assumed to be located in the corn belt of the USA, with centralized units for processing corncobs transported from several suppliers. The method of Turton et al. [40] is employed for economic analysis of alternatives, with Fixed Capital Investment (*FCI*) estimated from equipment sizing accordingly to Campbell [41]. The Chemical Engineering Plant Cost Index (*CEPCI*) is used to update equipment costs, using 2017 as reference year (*CEPCI*=567.5). Premises for economic analysis are summarized in Table 8. Project lifetime of 23 years is assumed, considering 20 years of operation (as practiced for most chemical plants) after 03 years of construction, which provides the basis for comparison of the Net Present Value (*NPV*) of alternatives. *NPV* results for a shorter project lifetime of 10 years are also discussed.

Table 8. Economic premises for estimating capital investment and manufacturing cost (base scenario).

Item	Type	Value	Unit
Biomass	Raw material	50	US$/t
Electricity	Product	0.1087 [a]	US$/kWh
Methanol	Product	400	US$/t
Bio-oil	Product	18	US$/GJ
Biochar	Product	20	US$/t
Cooling-water	Utilities	0.016	US$/t
Demineralized water	Utilities	0.793	US$/t
Monoethanolamine	Utilities	1500	US$/t
Methanol catalyst	Utilities	200	US$/kg
Catalyst lifetime	Parameter	05	years
Construction years	Parameter	03	years
Project lifetime	Parameter	23	years
Annual interest rate	Parameter	10	%
Taxation rate	Parameter	34	%

[a] EIA, U.S. Energy Information Administration, Electric Power Monthly, available on: https://www.eia.gov/electricity/monthly/epm_table_grapher.php?t=epmt_5_6_a

The biomass purchase price is based on Maung and Gustafson [42], which report an existent commercial contract with corncob costing ≈US$50/t. Bio-oil base price is assumed at US$18/GJ (≈US$2.16 /gasoline-gallon-equivalent) [43]. Due to high uncertainty of bio-oil price, a sensitivity analysis is performed evaluating its impact on economic performance.

Biochar product is priced at US$20/t in accordance with Brown et al. [44]. All raw materials
and product prices are assumed at factory gate.

For comparison of economic performances, this work proposes a metric composed by the
NPV of alternatives at the end of project lifetime (23 years) – the Relative NPV (NPVREL) –
defined in Eq. (2), where superscripts GASIF, PYROL and COMB designate the three
evaluated processes.

$$NPVREL = \frac{NPV^{GASIF} - NPV^{PYROL}}{NPV^{COMB}} \qquad (2)$$

The composite index allows building maps in the space of product prices, depicting regions
of dominance of the technologies, where, for positive NPV^{COMB}, a positive *NPVREL* points to
superior performance of GASIF over PYROL.

3. Results and Discussion

Sec. 3.1 firstly presents results of biomass characterization, while process simulation results
comparing the three biomass conversion alternatives are presented and discussed in Sec. 3.2;
details concerning economic analyses are addressed in Sec. 3.3.

3.1. Biomass Characterization

One of the main problems when studying biomass feedstock is the requirement of proper
characterization, preferably on the basis of few lumped components [34]. In this study,
although not shown, several combinations of model components were investigated to
reproduce the experimental elemental composition reported by Zhang et al [29]. Validation
was performed by comparing the calculated against the experimental biomass LHV [29]. The
resulting compositional model with the exact values of the targeted reduced formula
($CH_{1.554}N_{0.006}O_{0.824}$) and best agreement with corncob LHV (15.79 MJ/kg, dry ash-free basis,
exhibiting -2.46% deviation) is presented in Table 9, and is used to simulate the three
alternative routes (GASIF, PYROL and COMB).

Table 9. Biomass compositional model results (ash-free).

Model Compounds	Chemical Formula	Mass Fraction
Anthracene	$C_{14}H_{10}$	0.0264
Maleic anhydride	$C_4H_2O_3$	0.1252
Pyridazine	$C_4H_4N_2$	0.0088
Sucrose	$C_{12}H_{22}O_{11}$	0.7532
Water	H_2O	0.0864

3.2. Energy Analysis

Table 10 displays the main simulation results with product flowrates and utilities demands. GASIF shows biomass-to-methanol conversion of 0.3755 kg methanol / kg biomass, corresponding to 53.14% recovery of biomass heating value (*%EnergyOut*, based on LHVs of methanol and biomass), while exporting 3.72 MW of surplus electricity. COMB presents advantage of efficient transportation of biomass energy by transmission lines producing 114.10 MW (Table 10) of electricity with net efficiency of 30.2%LHV. Despite of its simplicity, by including the makeup water need to operate a semi-closed cooling-tower system, this alternative has the highest consumption of water (271.0 t/h) due to the high heat duty of the Rankine vacuum condenser.

The bio-oil production from PYROL (28.71 t/h) shows 38.4% for *%EnergyOut*, based on $LHV_{Bio\text{-}oil}$=18.22 MJ/kg. Despite having the steam turbine of lowest capacity among the process alternatives, as this process has only pumps and compressors of low power consumption (Table 10), it exports more electricity than GASIF (7.85 MW). PYROL is also the process of lowest water consumption (64.3 t/h). Reduced machinery use in PYROL should also imply in increased competitiveness against GASIF and COMB as process scale is reduced, due to typically lower efficiency of small-sized equipment.

In mass ash-free basis, the fast pyrolysis biochar has elemental composition of 65.77%C, 5.03%H, 0.51%N, 28.69%O ($CH_{0.911}N_{0.006}O_{0.327}$), being in the composition range of lignite when plotted in a Van Krevelen (C-H-O) diagram [45], with the ash content being 8.41%w. For the purpose of estimating the biochar LHV, the same model components employed to represent biomass are used, with composition fitted to meet biochar chemical formula, resulting in $LHV_{Biochar}$=24.75 MJ/kg (ash-free). Fig. 5 presents a comparison of energy densities in volume basis of biomass and products.

Table 10. Main simulation results.

Item	Type	GASIF	COMB	PYROL	Unit
Biomass feed [a]	Raw material	96.81	96.81	96.81	t/h
Biomass LHV		377.8	377.8	377.8	MW
Methanol production	Product	36.35	-	-	t/h
Methanol purity		99.85	-	-	%w/w
Methanol LHV		200.8	-	-	MW
%EnergyOut		53.14	-	-	%
Bio-oil production	Product	-	-	28.71	t/h
Bio-oil purity		-	-	14.2	%w/w H_2O
Bio-oil LHV		-	-	145.2	MW
%EnergyOut		-	-	38.4	%
Biochar production [a]	Product	-	-	24.34	t/h
Biochar LHV		-	-	153.3	MW
%EnergyOut		-	-	40.6	%
Electricity exported	Product	3.72	114.10	7.85	MW
Power generation		18.52	116.66	8.35	MW
Power demand		14.80	2.57	0.51	MW
CO_2-rich gas production	Byproduct	31.54	-	-	t/h
CO_2 purity		98.2	-	-	%w/w
Water consumption [b]	Utility	162.3	271.0	64.3	t/h
MEA consumption	Utility	2.45	-	-	kg/h
Catalyst load [c]	Utility	29.61	-	-	t

[a] Including ash; [b] Both process water and cooling-water make-up; [c] Replacement every 5 years.
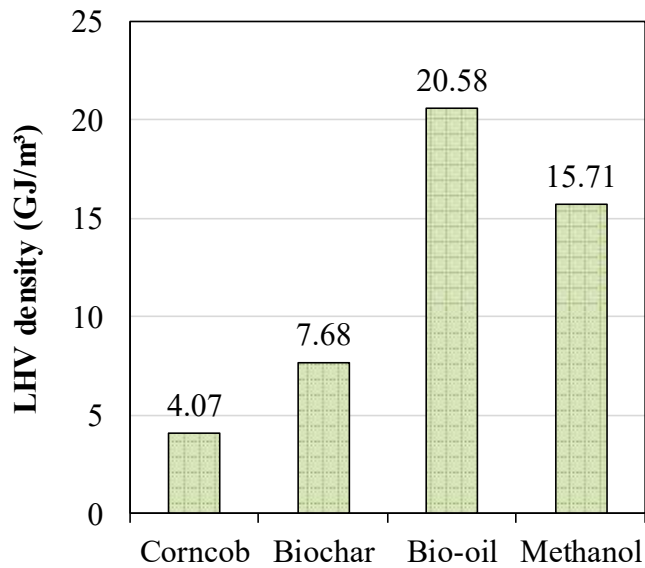
Fig. 5. Energy densities of biomass and products (LHV basis).

The energy densities signalize possible gains in transportation costs by implementing GASIF and PYROL, where the considered bulk densities are 290 kg/m³ for grinded corncob [6], 370 kg/m³ for biochar powder [46], 1130 kg/m³ for bio-oil and 790 kg/m³ for methanol (both from simulation, at ≈25°C). Bio-oil presents the highest LHV density (20.58 GJ/m³), providing densification of biomass energy (4.07 GJ/m³) and biochar production (7.68 GJ/m³). With these products, PYROL reduces 72.7% of the original biomass volume. GASIF allows 86.2% of volumetric reduction, with extra advantage of producing a single stable liquid product already in commercial purity, favoring transportation and storage logistics, but with reduced biomass energy recovery (*%EnergyOut*, Table 10). On the other hand, COMB eliminates the need for mass transportation but emits to the atmosphere the totality of the corncob carbon as CO_2. Fig. 6 depicts, for each thermochemical alternative, the destination distribution of corncob carbon among products.
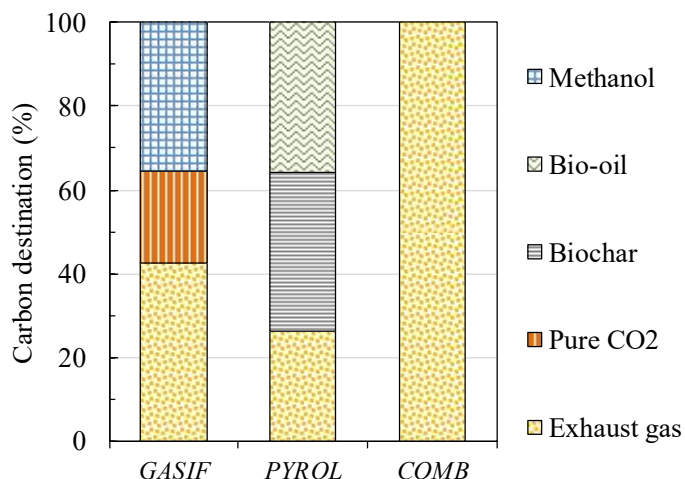
Fig. 6. Corncob carbon destination among products in each thermochemical process.

While COMB has 100% of corncob carbon being emitted in useless flue gas, GASIF produces 31.54 t/h of CO_2-rich gas (95.72%CO_2, 4.17%H_2O, 0.08%H_2, 0.03%CO in molar basis) that is emitted to the atmosphere. Should corn agricultural life-cycle impacts be allocated in the use of both grains and cobs [47], CO_2-rich gas could be sent to BECCS or industrial consumer, after proper conditioning (compression, dehydration and purification, if necessary), rendering GASIF nearly carbon-neutral. In GASIF, CO_2-rich gas byproduct carries 22.0% of corncob carbon, while methanol recovers 35.4%, with the remaining 42.6% being emitted through flue gas, totaling 90.9 t/h of emitted CO_2 (64.6%).

The bio-oil exported in PYROL carries 35.7% of corncob carbon, which is very similar to the carbon recovered as methanol in GASIF. In PYROL, biochar takes a larger share of the carbon input (38.0%), with the remaining 26.3% being emitted in flue gas. These aspects indicate that besides presenting higher energy recovery (Table 10), PYROL has superior performance concerning the utilization of biomass carbon (Fig. 6).

3.3. Economic Assessment

The detailed comparison of fixed capital investment (*FCI*) of process alternatives is presented in Fig. 7, discriminated by equipment types, with biomass converters showing the largest *FCI*

share. PYROL has the lowest *FCI*, followed by COMB and GASIF, resulting from employing fewer process machines, with low power consumption, and much smaller reactors for biomass conversion.

GASIF, on the other hand, requires installation of a complex plant with two thermochemical converters of relatively large dimensions including extra expenses with CO_2 separation from syngas, and methanol synthesis and purification. Significant contribution from heat exchangers, compressors and pumps stands out in *FCI* of GASIF (Fig. 7) mainly due to the high number of heat exchangers – many of them designed for high pressure application or operation with corrosive fluids (including aqueous MEA).
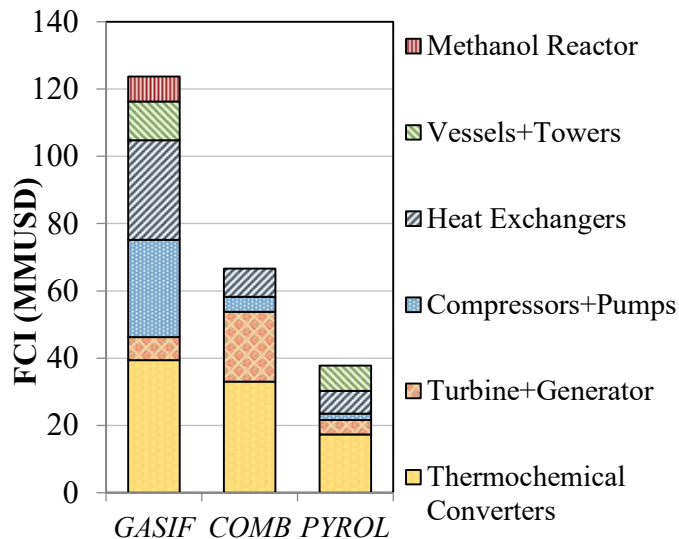
Fig. 7. Fixed capital investment (*FCI*) of process alternatives.

Additionally, syngas compression requires high pressure ratio and power input (quoted as two motor-driven shafts with five compression stages). In GASIF, biomass thermochemical conversion is $\approx 1/3$ of FCI^{GASIF}, while in COMB and PYROL it represents $\approx 1/2$ of *FCI*.

Table 11 displays the economic performance of the process alternatives in the base scenario (refer to Table 8). GASIF has best profitability – *NPV* is 118.74 MMUSD in the end of project horizon (20 operational years) – despite presenting the highest *FCI*. COMB is next, with final *NPV* of 110.32 MMUSD. This result is a consequence of GASIF exhibiting the

greatest annual profit (*AP*) of 35.29 MMUSD/y against 25.97 MMUSD/y and 21.01

MMUSD/y, of COMB and PYROL, respectively. This is mainly due to its superior revenues

(*REV*) from methanol sales, whereas GASIF has *REV* of 119.56 MMUSD/y (20.5% above

COMB *REV*) and PYROL has *REV* 13.6% below COMB *REV*.

Table 11. Economic performance of alternatives in the base scenario.

Item	GASIF	COMB	PYROL	Unit
Fixed Capital Investment (*FCI*)	123.76	66.65	37.92	MMUSD
Cost of Manufacturing (*COM*)	72.47	63.30	55.81	MMUSD/y
Revenues (*REV*)	119.56	99.22	85.69	MMUSD/y
Cost of Raw Material (*CRM*)	38.72	38.72	38.72	MMUSD/y
Cost of Utilities (*CUT*)	1.61	2.63	0.624	MMUSD/y
Gross Annual Profit (*GAP*)	47.09	35.91	29.88	MMUSD/y
Annual Profit (*AP*)	35.29	25.97	21.01	MMUSD/y
Payback Time [a]	9	7	6	years
Net Present Value (*NPV*)				
10 years of project lifetime	23.08	38.83	44.88	MMUSD
23 years of project lifetime	118.74	110.32	102.62	MMUSD

[a] Including 03 years of construction.

The cost of manufacturing (*COM*) increases from PYROL to COMB and to GASIF. All

routes have equal Cost of Raw Material (*CRM*) since the same amount of corncob (the only

required raw material) is used for comparison purposes. Cost of Utilities *(CUT)* changes

significantly, but with little influence on the final performance, mainly resulting from

differences in cooling-water duties and process makeups (MEA and water in GASIF).

Expenses with the methanol catalyst are not included in the *CUT* value reported in Table 11

but are applied for every 05 years of operation campaign.

In terms of payback time, processes with lowest *FCI* have superior performances, with

PYROL being the alternative of best short-term profitability followed by COMB (Table 11).

This is also shown in Fig. 8, which presents *NPV* profiles of GASIF, COMB and PYROL for

23 years of project lifetime, in the base scenario. The initial sequences of bars express the

construction years, where GASIF has the lowest NPVs due to its higher FCI. PYROL starts to present positive NPV at the 6th year of project (3rd year of operation), while COMB payback occurs one year later and GASIF only at the 9th year. Supported by the greater annual profits of COMB and GASIF, Fig. 8 shows that NPV^{COMB} first surpass NPV^{PYROL} at the 14th year, with NPV^{GASIF} overcoming them 3 years later.
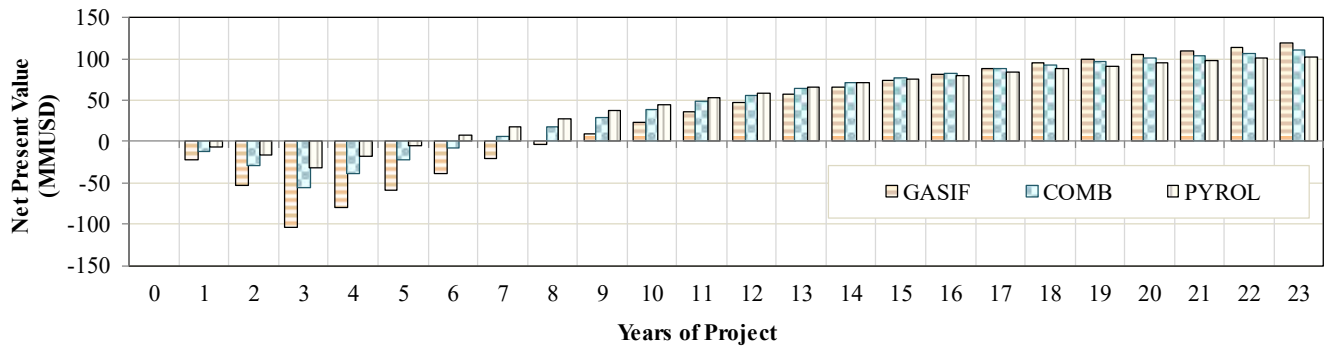
Fig. 8. Net present value of process alternatives along project lifetime.

In a shorter horizon of 10 years, Table 11 and Fig. 8 show inversely ranked NPV compared to project end, expressing midterm dominance of FCI (Fig. 7) and indicating the instantly best performance of PYROL, 44.88 MMUSD NPV after 10 years, against 38.83 and 23.08 MMUSD in COMB and GASIF, respectively. Differently from process revenues, which grow linearly with process scale, capital costs benefit from enlarging process scale – FCI growth factor follows approximately a 0.6 power law with the capacity factor [40]. Consequently, processes exhibiting high FCI are favored by large scale, and the observed gradual economic advantage of GASIF and COMB over PYROL (Fig. 8) would be considerably lowered by reducing process scales. In addition to longer payback being expected, COM would also be impaired to a little extent at reduced scales in accordance with the applied method [40]. It means that the higher FCI of GASIF and COMB alternatives could hamper their economic advantage if profits were not sufficiently high. The assumed scale of processing 96.81 t/h of corncob favors the most capital-intensive routes (Fig.7).

Sensitivity analyses on payback time of alternatives are presented in Fig. 9 for variable prices of biomass (Fig. 9a) and products (Fig. 9b).
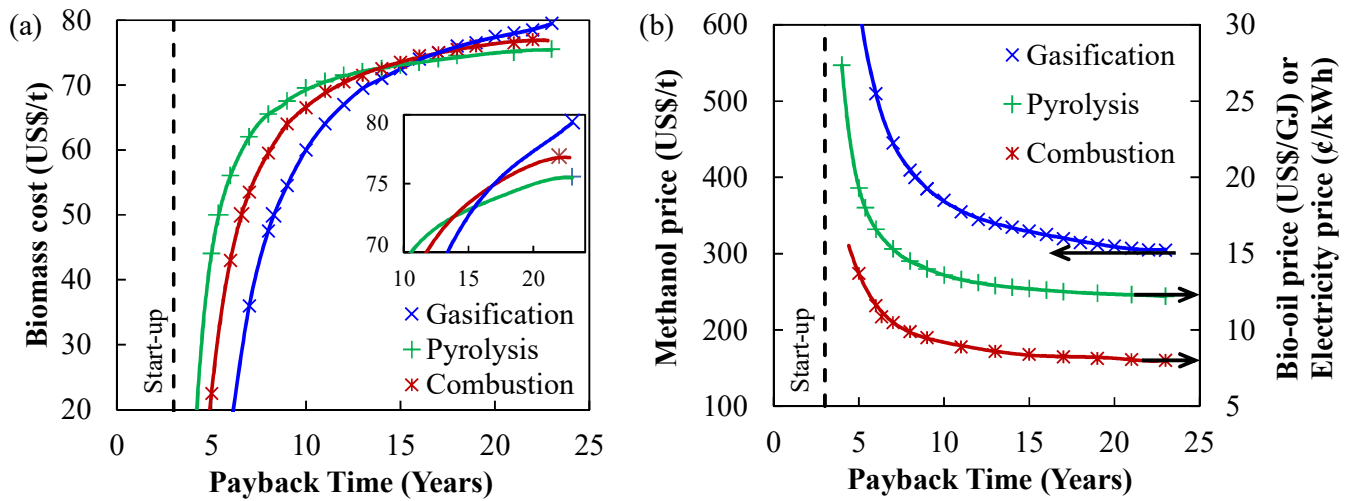
Fig. 9. Influence of payback time (in years): (a) biomass cost, and (b) product prices.

PYROL (Fig. 9a) presents the fastest payback (13 years) as long as biomass cost is lower than ≈ US$72/t , which may be a plausible value for best profitability and interest of farmers in the US scenario [48]. For higher biomass cost, alternatives with higher revenues (COMB and GASIF) overcome PYROL before reaching a null *NPV* (Fig. 9a). Fig. 9a shows that the maximum allowable corncob prices yielding positive *NPV* in the end of project lifetime are 79.5, 77.4 and 75.5 US$/t, respectively for GASIF, COMB and PYROL. Hence, the thermochemical alternatives for corncob processing would be unfeasible in the base scenario if the price of grinded biomass were above US$80/t. Fig. 9b shows that the minimum allowable product prices for attractiveness of GASIF, COMB and PYROL are US$303/t methanol, US$80.1/MWh electricity and US$12.2/GJ bio-oil (≈US$1.47/gasoline-gallon-equivalent).

Table 12 shows economic performances and minimum allowable product prices for the investigated routes under three biomass cost scenarios – 30, 50 and US$70/t, showing that GASIF outperforms the other alternatives, regardless of biomass cost, provided the product prices of the base scenario are constant.

Table 12. Economic performance of alternatives for different biomass costs.

Item	Low	Base	High	Unit
Biomass Purchase Cost	30	50	70	US$/t
Net Present Value (*NPV*) [a,b]				
GASIF	199	118	38	MMUS$
COMB	191	110	30	MMUS$
PYROL	183	103	22	MMUS$
Payback Time [b,c]				
GASIF	7	9	14	years
COMB	6	7	12	years
PYROL	5	6	11	years
Minimum Product Price				
GASIF / Methanol	238	303	369	US$/t
COMB / Electricity	59.2	80.1	101	US$/MWh
PYROL / Bio-oil	7.63	12.2	16.7	US$/GJ

[a] *NPV* at the end of 23 years of project; [b] Products at base prices; [c] Including 03 years of construction

Table 12 complements Fig. 9a with economic analysis results for variable biomass cost. At the high-price of US$70/t, the final NPVs for the evaluated alternatives (*NPV* at the end of the project, including interest rate of 10%) are positive, though lower than *FCI*. Therefore, the mid- to long-term payback of alternatives show that, although the processes are feasible, their attractiveness is low. On the other hand, biomass at US$30/t renders very attractive the scenario, allowing low minimum product prices and short-term payback of investments. Such low price may be difficult to attain due to handling, grinding and transporting costs.

Fig. 10 displays a comparative sensitivity analysis of profitability for the three routes through the Relative NPV (*NPVREL*) defined in Eq. (2).
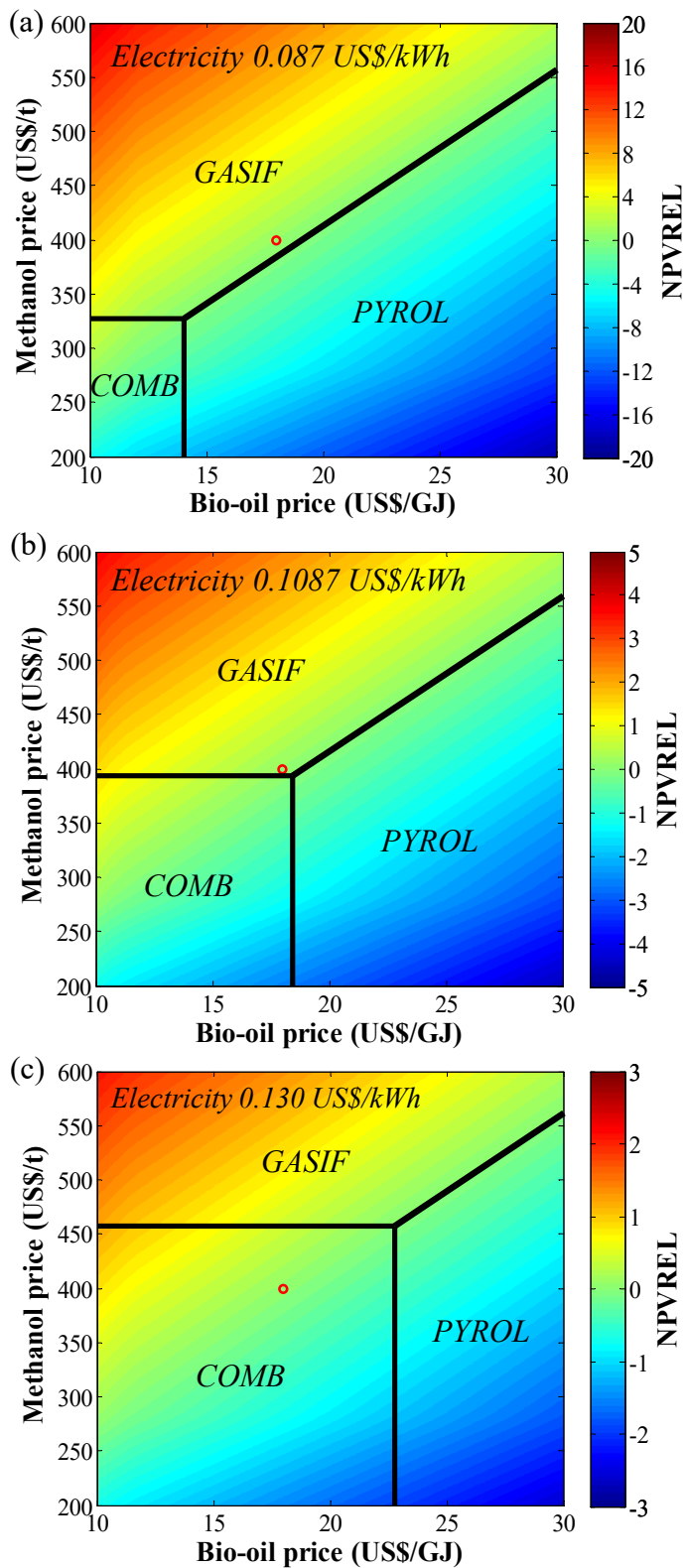
Fig. 10. Relative net present value (*NPVREL*) for variable product prices and indication of the most profitable process alternative in different energy scenarios: (a) low-priced electricity at US$87/MWh (-20%); (b) base price of US$108.7/MWh; and (c) high-priced electricity at US$130/MWh (+20%). The circle indicates performance with methanol and bio-oil base prices, highlighting the movement of the profitability frontier with electricity price (*GASIF*=Gasification; *COMB*=Combustion; *PYROL*=Pyrolysis).

The analysis explores sensitivity to variable product prices at three electricity prices – 87.0 (Fig. 10a), 108.7 (Fig. 10b) and 130.0 US$/MWh (Fig. 10c) – indicating regions of dominant performance of the alternatives in the plane bio-oil versus methanol prices. Positive values mean GASIF outperforming PYROL. The frontiers of COMB dominance region are determined by product prices giving the same final NPV (23 years of project). A circle is drawn to indicate performance at methanol and bio-oil base prices (US$400/t methanol and US$18/GJ bio-oil), highlighting the movement of the profitability frontier with electricity price. Figs. 9b, 10a and10c are complementary to each other regarding the economic performance of alternatives.

Fig. 10a presents a relatively small region of COMB route, far from the base point circle, with GASIF unveiling best profitability since, in such scenario, equal $NPVs$ are achieved with US$327/t methanol and US$14.0/GJ bio-oil. In Fig. 10b (electricity base price), COMB zone approaches the base scenario circle – also located in GASIF region – indicating proximity of $NPVs$, which equalizes at US$393/t methanol and US$18.4/GJ bio-oil. Only in Fig. 10c COMB clearly outperforms GASIF and PYROL as their frontiers move to US$458/t methanol and US$22.8/GJ bio-oil.

Despite revealing best $NPVs$ at the base scenario, GASIF may be vulnerable to product price fluctuation, since methanol price – considered at US$400/t, 30% above the minimum (Fig. 9b) – typically ranges from 200 to 500 US$/t with high volatility. Besides no longer being the alternative of highest NPV for methanol prices below ≈US$350 (Fig. 10), fluctuations below US$305/t methanol could hamper the investment payback (Fig. 9b). However, GASIF profitability can be enhanced through monetization (e.g. BECCS with enhanced oil recovery or CO_2 conversion to chemicals) of the CO_2-rich gas obtained from syngas upgrading, after appropriate conditioning. For instance, if CO_2-rich gas is monetized at only US$10/t, GASIF remains economically feasible even with methanol at US$288/t.

With less price volatility, as long as the average electricity price remains above US$87/MWh, COMB is the safest investment, besides the lowest process complexity among the investigated alternatives. Furthermore, COMB avoids transportation and storage costs, while being the most advantageous above 108.7/MWh (Fig. 10), presenting mid-term payback and great profitability potential (Table 11). Compared to GASIF, COMB has also the advantage of much better flexibility for plant start-up and shutdown, with reduced associated expenses.

PYROL, besides presenting the lowest payback time (Fig. 9) due to low FCI (Fig. 7), reveals good potential of NPV competitiveness (Fig. 10), but bio-oil price above US$18/GJ is necessary to overcome GASIF performance. For instance, sale of bio-oil to upgrading refineries in the US scenario makes the end-user price for home heating uncompetitive to replace fuel oil #2, currently priced at about US$10.5/GJ (≈US$2/gal) for resellers purchase. Even considering that upgraded bio-oil could be blended with commercial fuel oils, to minimize the impact on wholesale price, PYROL should receive biomass at reduced cost. In this sense, Table 12 reveals an attractive minimum allowable bio-oil price of US$7.6/GJ for biomass costing US$30/t, but, even in this case, the NPV^{GASIF} should overcome NPV^{PYROL}. Biochar sales would hardly contribute to effectively improve AP^{PYROL} since it has small participation on REV^{PYROL}, so that it would be necessary to duplicate the biochar price (US$40/t) to make NPV^{PYROL} higher than NPV^{COMB}, meaning that PYROL would still be less profitable than GASIF. Contrarily, with bio-oil priced at US$18/GJ and biochar at US$20/t it would be necessary to increase the considered interest rate from 10% to 16% to make NPV^{PYROL} overcome the NPV of other alternatives assisting its rapid payback due to low FCI^{PYROL}. Therefore, despite of the highest energy recovery and LHV density of its products, and the lowest FCI, the economic results at the base scenario indicate PYROL as the least attractive route among the considered alternatives.

4. Conclusions

In this work, three thermochemical pathways – gasification (GASIF), combustion (COMB) and fast pyrolysis (PYROL) – for corncob transformation into energy products – methanol, electricity and bio-oil – are investigated from a process systems engineering perspective comparing their energy and economic performances.

The energy densification potential of GASIF and PYROL are evaluated in terms of biomass volume reductions of 86.2% and 72.7%, respectively. GASIF has the advantage of producing a single stable liquid product already in commercial purity, favoring transportation and storage logistics, but with reduced energy recovery. Expressed as recovery of biomass LHV in products, GASIF shows 53.14% in methanol, while PYROL presents 38.4% in bio-oil and 40.6% in biochar. COMB has the advantage of total volume reduction and the biomass-fueled power plant presents net efficiency of 30.2%LHV.

From the perspective of destination of corncob carbon, GASIF and PYROL avoid CO_2 emissions by 35.4% and 73.7%, respectively, through chemical storage in its corresponding products. Singularly, in the GASIF process, CO_2-rich gas (nearly pure CO_2) could be recovered as byproduct – from syngas upgrading carrying 22% of carbon feed – though this study adopts venting it to the atmosphere. Should it be dispatched for storage (a BECCS application) or for industrial utilization after appropriate conditioning, emission avoidance of 57.4% could be attained. However, even in such scenario, PYROL presents superior performance concerning the utilization of biomass carbon. Further research might explore the entire upstream and downstream chain to determine the carbon footprint though a full Life Cycle Assessment, as transport stage is not considered.

The economic analysis shows that all process alternatives present positive net present value by the end of project lifetime, as long as the biomass cost is below US\$75.5/t. PYROL is the alternative with fastest payback as it requires the lowest fixed capital investment, though

exhibiting the lowest long-term profitability. High bio-oil price above US$18/t would be necessary to have PYROL outperforming other alternatives. In this sense, GASIF is the most profitable route, though presenting the highest vulnerability to product price volatility. Its profitability is followed by the COMB alternative, which advantageously bears operational and construction simplicity.

Acknowledgements

Abbreviations

BECCS Bio-Energy with Carbon Capture and Storage; BTL Biomass-to-Liquids; ¢ US Dollar Cents; COMB Biomass Combustion Route; DCC Direct Contact Column; EOS Equation-of-State; GASIF Biomass Gasification Route; LHV Lower Heating Value; MEA Monoethanolamine; PR Peng-Robinson; PYROL Biomass Fast Pyrolysis Route; ST Steam Turbine; USD US Dollars.

Nomenclature

%EnergyOut   *: Percentage of corncob energy input on LHV basis (unitless);*
AP, GAP   *: Annual profit and gross profit (USD/y);*
CEPCI   *: Chemical engineering plant cost index (unitless);*
COM   *: Annual cost of manufacturing (USD/y);*
CRM, CUT   *: Annual utility and raw material costs (USD/y);*
FCI   *: Fixed capital investment (USD);*
LHV   *: Lower heating value (MJ/kg);*
NPV   *: Net present value (USD);*
NPVREL   *: Relative net present value (unitless);*
REV   *: Revenues (USD/y);*
S   *: Methanol synthesis coefficient (unitless).*

References

[1] W. Zhang, Automotive fuels from biomass via gasification, Fuel Process. Technol. 91 (2010) 866–876. https://doi.org/10.1016/j.fuproc.2009.07.010

[2] E. Johnson, Goodbye to carbon neutral: getting biomass footprints right, Environ. Impact Assess. Rev. 29 (2009) 165–168. https://doi.org/10.1016/j.eiar.2008.11.002.

[3] R. Contreras-Lisperguer, E. Batuecas, C. Mayo, R. Díaz, F.J. Pérez, C. Springer, Sustainability assessment of electricity cogeneration from sugarcane bagasse in Jamaica, J. Clean. Prod. 200 (2018) 390–401. https://doi.org/10.1016/j.jclepro.2018.07.322

[4] M.O.S. Dias, M. Modesto, A.V. Ensinas, S.A. Nebra, R. Maciel Filho, C.E.V. Rossell, Improving bioethanol production from sugarcane: evaluation of distillation, thermal integration and cogeneration systems, Energy 36 (2011) 3691–3703. https://doi.org/10.1016/j.energy.2010.09.024

[5] P. Gallagher, G. Schamel, H. Shapouri, H. Brubaker, The international competitiveness of the U.S. corn-ethanol industry: a comparison with sugar-ethanol processing in Brazil. Agribus. 22 (2006) 109–134. https://doi.org/10.1002/agr.20072.

[6] N. Kalyian, R.V. Morey, Densification characteristics of corn cobs, Fuel Process. Technol. 91 (2010) 559–565. https://doi.org/10.1016/j.fuproc.2010.01.001

[7] C. Jansen, T. Lübberstedt, Turning maize cobs into a valuable feedstock, Bioenerg. Res. 5 (2012) 20–31. https://doi.org/10.1007/s12155-011-9158-y

[8] X. Liu, Y. Zhang, Z. Li, R, Feng, Y. Zhang, Characterization of corncob-derived biochar and pyrolysis kinetics in comparison with corn stalk and sawdust, Bioresour. Technol. 170 (2014) 76–82. https://doi.org/10.1016/j.biortech.2014.07.077.

[9] Y. Li, T. Wang, X. Yin, C. Wu, L. Ma, H. Li, Y. Lv, L. Sun, 100 t/a-Scale demonstration of direct dimethyl ether synthesis from corncob-derived syngas, Renew. Energ. 35 (2010) 583–587. https://doi.org/10.1016/j.renene.2009.08.002

[10] N.S. Shamsul, S.K. Kamarudin, N.A. Rahman, N.T. Kofli, An overview on the production of bio-methanol as potential renewable energy, Renew. Sustain. Energ. Rev. 33 (2014) 578–588. https://doi.org/10.1016/j.rser.2014.02.024

[11] K.T. Malladi, T. Sowlati, Biomass logistics: a review of important features, optimization modeling and the new trends, Renew. Sustain. Energ. Rev. 94 (2018) 587–599. https://doi.org/10.1016/j.rser.2018.06.052.

[12] J.S. Tumuluru, C.T. Wright, J.R. Hess, K.L. Kenney, A review of biomass densification systems to develop uniform feedstock commodities for bioenergy application, Biofuels Bioprod. Bioref. 5 (2011) 683–707. https://doi.org/10.1002/bbb.324.

[13] J.S. Tumuluru, C.T. Wright, K.L. Kenney, J.R. Hess, A review on biomass densification technologies for energy application, INL/EXT-10-18420, Idaho National Laboratory (INL), Biofuels and Renewable Energy Technologies Department, Energy Systems and Technologies Division, Idaho Falls, Idaho 83415, August 2010. https://doi.org/10.2172/1016196

[14] C.A. García, R. Betancourt, C.A. Cardona, Stand-alone and biorefinery pathways to produce hydrogen through gasification and dark fermentation using *Pinus patula*, J. Environ. Manag. 203 (2017) 695–703. https://doi.org/10.1016/j.jenvman.2016.04.001

[15] O. Onay, O.M. Kockar, Slow, fast and flash pyrolysis of rapeseed, Renew. Energ. 28 (2003) 2417–2433. https://doi.org/10.1016/S0960-1481(03)00137-X.

[16] Z. Chen, M. Wang, E. Jiang, D. Wang, K. Zhang, Y. Ren, Y. Jiang, Pyrolysis of torrefied biomass, Trends Biotechnol. 36 (2018) 1287–1298. https://doi.org/10.1016/j.tibtech.2018.07.005.

[17] A.V. Bridgwater, Review of fast pyrolysis of biomass and product upgrading, Biomass Bioenerg. 38 (2012) 68–94. https://doi.org/10.1016/j.biombioe.2011.01.048

[18] P.C. Badger, P. Fransham, Use of mobile fast pyrolysis plants to densify biomass and reduce biomass handling costs – a preliminary assessment, Biomass Bioenerg. 30 (2006) 321–325. https://doi.org/10.1016/j.biombioe.2005.07.011.

[19] K. Lazdovica, L. Liepina, V. Kampars, Comparative wheat straw catalytic pyrolysis in the presence of zeolites, Pt/C, and Pd/C by using TGA-FTIR method, Fuel Process. Technol. 138 (2015) 645–653. https://doi.org/10.1016/j.fuproc.2015.07.005

[20] M.B. Shemfe, S. Gu, P. Ranganathan, Techno-economic performance analysis of biofuel production and miniature electric power generation from biomass fast pyrolysis and bio-oil upgrading, Fuel 143 (2015) 361–372. http://doi.org/10.1016/j.fuel.2014.11.078

[21] M. Gholizadeh, R. Gunawan, X. Hu, S. Kadarwati, R. Westerhof, W. Chaiwat, M. Hasan, C.Z. Li, Importance of hydrogen and bio-oil inlet temperature during the hydrotreatment of bio-oil, Fuel Process. Technol. 150 (2016) 132–140. https://doi.org/10.1016/j.fuproc.2016.05.014

[22] T. Yang, L. Shi, R. Li, B. Li, X. Kai, Hydrodeoxygenation of crude bio-oil in situ in the bio-oil aqueous phase with addition of zero-valent aluminum, Fuel Process. Technol. 184 (2019) 65–72. https://doi.org/10.1016/j.fuproc.2018.10.025

[23] M. Sharifzadeh, M. Sadeqzadeh, M. Guo, T.N. Borhani, N.V.S.N.M. Konda, M.C. Garcia, L. Wang, J. Hallett, N. Shah, The multi-scale challenges of biomass fast pyrolysis and bio-oil upgrading: review of the state of art and future research directions, Prog. Energ. Combust. Sci. 71 (2019) 1–80. https://doi.org/10.1016/j.pecs.2018.10.006

[24] Q. Xiong, Y. Yang, F. Xu, Y. Pan, J. Zhang, K. Hong, G. Lorenzini, S. Wang, Overview of computational fluid dynamics simulation of reactor-scale biomass pyrolysis, ACS Sustain. Chem. Eng. 5 (2017) 2783–2798. https://doi.org/10.1021/acssuschemeng.6b02634

[25] Q. Xiong, F. Xu, Y. Pan, Y. Yang, Z. Gao, S. Shu, K. Hong, F. Bertrand, J. Chaouki, Major trends and roadblocks in CFD-aided process intensification of biomass pyrolysis, Chem. Eng. Process. 127 (2018) 206–212. https://doi.org/10.1016/j.cep.2018.04.005

[26] F. Trippe, M. Fröhling, F. Schultmann, R. Stahl, E. Henrich, Techno-economic analysis of fast pyrolysis as a process step within biomass-to-liquid fuel production, Waste Biomass Valor. 1 (2010) 415–430. https://doi.org/10.1007/s12649-010-9039-1

[27] H. Zhang, R. Xiao, H. Huang, G. Xiao, Comparison of non-catalytic and catalytic fast pyrolysis of corncob in a fluidized bed reactor, Bioresour. Technol. 100 (2009) 1428–1434. https://doi.org/10.1016/j.biortech.2008.08.031

[28] H. Zhang, R. Xiao, D. Wang, Z. Zhong, M. Song, Q. Pan, G. He, Catalytic fast pyrolysis of biomass in a fluidized bed with fresh and spent fluidized catalytic cracking (FCC) catalysts, Energ. Fuels 23 (2009) 6199–6206. https://doi.org/10.1021/ef900720m

[29] H. Zhang, R. Xiao, D. Wang, G. He, S. Shao, J. Zhang, Z. Zhong, Biomass fast pyrolysis in a fluidized bed reactor under N_2, CO_2, CO, CH_4 and H_2 atmospheres, Bioresour. Technol. 102 (2011) 4258–4264. https://doi.org/10.1016/j.biortech.2010.12.075

[30] P. Basu, Biomass Gasification, Pyrolysis, and Torrefaction – Practical Design and Theory, second ed., Elsevier, San Diego, 2013.

[31] S. Amin, Review on biofuel oil and gas production processes from microalgae, Energ. Convers. Manag. 50 (2009) 1834–1840. https://doi.org/10.1016/j.enconman.2009.03.001.

[32] H. Boerrigter, R. Rauch, Review of applications of gases from biomass gasification, ECN Research, ECN-RX--06-066 (2006). https://www.ecn.nl/publicaties/PdfFetch.aspx?nr=ECN-RX--06-066.

[33] M.H. Rafiq, H.A. Jakobsen, R. Schmid, J.E. Hustad, Experimental studies and modeling of a fixed bed reactor for Fischer–Tropsch synthesis using biosyngas, Fuel Process. Technol. 92 (2011) 893–907. https://doi.org/10.1016/j.fuproc.2010.12.008.

[34] F. Manenti, F. Adani, F. Rossi, G. Bozzano, C. Pirola, First-principles models and sensitivity analysis for the lignocellulosic biomass-to-methanol conversion process, Comput. Chem. Eng. 84 (2016) 558–567. https://doi.org/10.1016/j.compchemeng.2015.05.012

[35] R.P. Anex, A. Aden, F.K. Kazi, J. Fortman, R.M. Swanson, M.M. Wright, J.A. Satrio, R.C. Brown, D.E. Daugaard, A. Platon, G. Kothandaraman, D.D. Hsu, A. Dutta, Techno-economic comparison of biomass-to-transportation fuels via pyrolysis, gasification, and biochemical pathways, Fuel 89 (2010) S29–S35. https://doi.org/10.1016/j.fuel.2010.07.015

[36] X. Zhao, T.R. Brown, W.E. Tyner, Stochastic techno-economic evaluation of cellulosic biofuel pathways, Bioresour. Technol. 198 (2015) 755–763. https://doi.org/10.1016/j.biortech.2015.09.056

[37] T.R. Brown, A techno-economic review of thermochemical cellulosic biofuel pathways, Bioresour. Technol. 178 (2015) 166–176. https://doi.org/10.1016/j.biortech.2014.09.053

[38] K. Hakouk, M. Klotz, E. Di Geronimo, V. Ranieri, J.A.Z. Pieterse, G. Aranda-Almansa, A.M. Steele, S. Thorpe, Implementation of novel ice-templated materials for conversion of tars from gasification product gas, Fuel Process. Technol. 181 (2018) 340–351. https://doi.org/10.1016/j.fuproc.2018.10.009

[39] M.A. Adnan, Q. Xiong, A. Hidayat, M.M. Hossain, Gasification performance of *Spirulina* microalgae – a thermodynamic study with tar formation, Fuel 241 (2019) 372–381. https://doi.org/10.1016/j.fuel.2018.12.061

[40] R. Turton, R.C. Bailie, W.B. Whiting, J.A. Shaeiwitz, D. Bhattacharya, Analysis, Synthesis, and Design of Chemical Processes, fourth ed., Prentice Hall, New Jersey, 2012.

[41] J.M. Campbell, Gas Conditioning and Processing, v. 2: The Equipment Modules, seventh ed., Campbell Petroleum Series, Norman/Oklahoma, 1984.

[42] T.A. Maung, C.R. Gustafson, The viability of harvesting corn cobs and stover for biofuel production in North Dakota, Proceedings of Agricultural & Applied Economics Association's 2011 AAEA & NAREA Joint Annual Meeting, Pittsburgh, Pennsylvania, July 24-26, 2011.

[43] M.M. Wright, J.A. Satrio, R.C. Brown, D.E. Daugaard, D.D. Hsu, Techno-economic analysis of biomass fast pyrolysis to transportation fuels, Technical Report, NREL/TP-6A20-46586, November 2010.

[44] T.R. Brown, Y. Zhang, G. Hu, R.C. Brown, Techno-economic analysis of biobased chemicals production via integrated catalytic processing, Biofuels Bioprod. Bioref. 6 (2012) 73–87. https://doi.org/10.1002/bbb.344

[45] J. Poudel, S. Karki, S.C. Oh, Valorization of waste wood as a solid fuel by torrefaction, Energies 11 (2018) 1641 https://doi.org/10.3390/en11071641

[46] I.M. Lima, A.A. Boateng, K.T. Klasson, Physicochemical and adsorptive properties of fast-pyrolysis bio-chars and their steam activated counterparts, J. Chem. Technol. Biotechnol. 85 (2010) 1515–1521. https://doi.org/10.1002/jctb.2461

[47] R. Frischknecht, Allocation in life cycle inventory analysis for joint production, Int. J. Life Cycle Assess. 5 (2000) 85–95. https://doi.org/10.1007/BF02979729.

[48] M.J. Erickson, C. Dobbins, W.E. Tyner, The economics of harvesting corn cobs for energy, Plant Manag. Netw. 10 (2011). https://doi.org/10.1094/CM-2011-0324-02-RS